Carbon Steel Wettability Characteristics Enhancement for Improved Enamelling Using a 1.2 kW High Power Diode Laser

J. Lawrence and L. Li

Laser Process Engineering Group, Manufacturing Division, Department of Mechanical Engineering, University of Manchester Institute of Science and Technology (UMIST), Manchester, M60 1QD, UK.

Correspondence

Dr. Jonathan Lawrence

Manufacturing Division,

Department of Mechanical Engineering,

University of Manchester Institute of Science and Technology (UMIST),

Manchester,

M60-1QD,

UK.

Tel : (44) (44) 161 236-3311

Fax : (44) 161 200-3803

e-mail : j.lawrence@stud.umist.ac.uk

ABSTRACT

High power diode laser (HPDL) surface treatment of a common engineering carbon steel (EN8) was found to effect significant changes to the wettability characteristics of the metal. These modifications have been investigated in terms of the changes in the surface roughness of the steel, the presence of any surface melting, the polar component of the steel surface energy and the relative surface oxygen content of the steel. The morphological and wetting characteristics of the mild steel and the enamel were determined using optical microscopy, scanning electron microscopy (SEM), X-ray photoemission spectroscopy (XPS), energy dispersive X-ray (EDX) analysis and wetting experiments by the sessile drop technique. This work has shown that HPDL radiation can be used to alter the wetting characteristics of carbon steel so as to facilitate improved enamelling.

Keywords: laser; steel; enamel; wettability; surface

1 INTRODUCTION

Both scientists and engineers alike have a great interest in understanding the interfacial phenomena between vitreous enamels and carbon steels, since in many practical applications where vitreous enamels are fired onto carbon steels, the performance of the article is directly linked to the nature of the enamel-steel interface. Many studies to investigate these phenomena have been carried out, however, they have been principally concerned with the wettability of zirconia and other oxide ceramics on metals [1-5] as well as the adhesion of silicone sealants to aluminium [6] and the coating of aluminium alloys with ceramic materials [7, 8]. The interfacial mechanisms investigated have centred principally around the thermodynamic criterion [2, 3, 5], the electronic theory [4] and the occurrence of oxidation [1, 9].

To date, very little published work exists pertaining to the use of lasers for altering the surface properties of materials in order to improve their wettability characteristics. Notwithstanding this, it is recognised within the currently published work that laser irradiation of a metal surface can bring about changes in the metal's wettability characteristics. Previously Zhou *et al.* [7, 8] carried out work on the laser coating of aluminium alloys with ceramic materials (SiO_2, Al_2O_3, etc.), reporting on the well documented fact that generated oxide layers often promote metal/oxide wetting. Further, Heitz *et al.* [10], Henari *et al.* [11] and Olfert *et al.* [12] have found that excimer laser treatment of metals results in improved coating adhesion. The improvements in adhesion were attributed to the fact that the excimer laser treatment resulted in a smoother surface and as such enhanced the action of wetting. However, the reasons for these changes with regard to changes in the material's surface morphology, surface composition and surface energy are not reported. In contrast, in a more comprehensive study by Lawrence *et al.* [13], which compared the effects of CO_2, Nd:YAG, excimer and high power diode laser (HPDL) radiation on the wettability characteristics of a mild steel, it was found that changes in the wettability characteristics of the steel varied depending upon the laser type.

This present work details the use of a novel 1.2 kW HPDL to alter the wettability characteristics of a common engineering carbon steel (EN8), and the effects thereof on the adhesion and bonding characteristics with a vitreous enamel. The intention being to facilitate the hitherto impossible task of enamelling carbon steel in normal atmospheric conditions without pre-treatment of the steel. Indeed, such a process has been employed by the authors to facilitate the sealing, by means of laser enamelling, of ceramic tile grouts [14-17].

2 THEORETICAL BACKGROUND

When a drop of liquid is in contact with a solid surface, the final shape taken by the drop, and thus whether it will wet the surface or not, depends upon the relative magnitudes of the molecular forces that exist within the liquid (cohesive) and between the liquid and the solid (adhesive) [18]. The index of this effect for an ideal surface is the contact angle, θ, which the liquid subtends with the solid. The adhesion intensity of a liquid to a solid surface is known as the work of adhesion, W_{ad}, and is related to the liquid surface energy, γ_{lv}, by the Young-Dupre equation:

$$W_{ad} = \gamma_{lv}(1+\cos\theta) \tag{1}$$

It is important to consider also the influence of the substrate surface roughness on the wetting contact angle. Rough grooves on a surface, which may contribute to the influence of contact angles, can be categorised as either radial or circular grooves. Any practical rough surface can be represented by a combination of these two cases [19]. In fact two roughness parameters can be defined: the Wenzel type, D_R [20] and the Cassie/Baxter type, F_R [21] In the case that wetting spreads radially, as is the likely case with the AOC, then the resulting radial contact angle, θ_{rad}, is related to the theoretical contact angle, θ_{th}, by

$$\cos\theta_{rad} = D_R\left(1-F_R\right)\cos\theta_{th} - F_R \tag{2}$$

According to Neumann [22], only if F_R is equal to zero, then a model similar to that for heterogeneous solid surfaces can be developed in order to account for surface irregularities, being given by Wenzel's equation:

$$r\left(\gamma_{sv}-\gamma_{sl}\right) = \gamma_{lv}\cos\theta_w \tag{3}$$

where r is the roughness factor defined as the ratio of the real and apparent surface areas and θ_w is the contact angle for the wetting of a rough surface. It is important to note that Wenzel's treatment is only effective at the position of wetting triple line [19]. Nevertheless, Eq. (3) shows clearly, the influence of surface roughness on the contact angle is to cause an increase in the contact angle. Thus, the smoother the contact surface is, then the smaller the contact angle will be.

The intermolecular attraction which is responsible for surface energy, γ, results from a variety of intermolecular forces whose contribution to the total surface energy is additive [23]. The majority of these forces are functions of the particular chemical nature of a certain material, and as such the total surface energy (γ) comprises of γ^p (polar or non-dispersive interaction) and γ^d (dispersive component). Therefore, the surface energy of any system may be described by [15]

$$\gamma = \gamma^d + \gamma^p \tag{4}$$

As such, W_{ad} can be expressed as the sum of the different intermolecular forces that act at the interface [23].

$$W_{ad} = W_{ad}^d + W_{ad}^p = 2\left(\gamma_{sv}^d \gamma_{lv}^d\right)^{1/2} + 2\left(\gamma_{sv}^p \gamma_{lv}^p\right)^{1/2} \tag{5}$$

By equating Eq. (5) with Eq. (1), the contact angle for solid-liquid systems can be related to the surface energies of the respective liquid and solid by

$$\cos\theta = \frac{2\left(\gamma_{sv}^d \gamma_{lv}^d\right)^{1/2} + 2\left(\gamma_{sv}^p \gamma_{lv}^p\right)^{1/2}}{\gamma_{lv}} - 1 \tag{6}$$

3 EXPERIMENTAL PROCEDURES

The laser used in the study was a 1.2 kW HPDL (Rofin-Sinar, DL-012), emitting at 940nm. The laser beam was focused directly onto the samples to a 6mm x 20mm rectangular beam with a fixed power of 500 W. The laser was operated in the continuous wave (CW) mode. The laser head assembly and focusing optics are shown schematically in Fig. 1. The beam was traversed across the samples by means of mounting the assembly head onto the z-axis of a 3-axis CNC table. The focused laser beam was thus fired across the surface of the mild steel by traversing the samples beneath the laser beam using the x- and y-axis of the CNC table at speeds of 250-2000 mm/min, whilst O_2 gas was pumped into a gas box in order to assist the surface treatment process.

The liquids used for the wetting experiments were human blood, human blood plasma, glycerol and 4-octanol. The test liquids, along with their total surface energy (γ_2) as well as the dispersive (γ_2^d) and polar (γ_2^p) components, are detailed in Table 1. An additional set of wetting experiments were

conducted to simply determine the contact angle between the enamel and the mild steel before and after laser treatment.

The solid materials used as substrates in the wetting experiments were rectangular billets (50 x 100mm with a thickness of 3mm) of common engineering low carbon mild steel (EN8). The contact surfaces of the materials were used as-received in the experiments. The enamel used commercially available enamel frit (Ferro) which, in order to form a manageable paste, was mixed with 20wt% white spirit. The composition of the enamel consisted mainly of the following; SiO_2, B_2O_3, Na_2O, Mn and small quantities of Pb, Ba, MgO, Al_2O_3 and Ni, whilst the powder size was less than 25μm medium size. The morphological and physical characteristics of the mild steel and the enamel were determined using optical microscopy, scanning electron microscopy (SEM), X-ray photoemission spectroscopy (XPS), energy dispersive X-ray (EDX) analysis.

The wetting experiments were carried out in atmospheric conditions at a temperature of 20^0C. The droplets were released in a controlled manner onto the surface of the mild steel substrate (treated and untreated) from the tip of a micropipette, with the resultant volume of the drops being approximately 6×10^{-3} cm^3. Each experiment lasted for three minutes with profile photographs of the sessile drops being obtained every minute, with the contact angle subsequently being measured. The experimental results showed that throughout the period of the tests no discernible change in the magnitude of the contact angle occurred.

4 RESULTS AND DISCUSSION

4.1 Enamel glaze characteristics

It was observed that, prior to laser irradiation, it was not possible to fire the enamel onto the as-received surface of the mild steel. Indeed, laser interaction with the enamel when placed on the untreated mild steel surface simply resulted in the 'balling' of the enamel (the formation of small spheres approximately the diameter of the laser beam itself). Such observations are in accord with those of Bourell *et al.* [24] and Agarwala *et al.* [25], who noted the balling phenomena during laser sintering work. After HPDL surface treatment of the mild steel, however, it was possible to fire the enamel directly onto the mild steel. The mechanism of this phenomena is based entirely on the wettability characteristics of the mild steel, as discussed later.

Fig. 2 shows the typical surface morphology of the HPDL fired enamel glaze on the mild steel. The glaze was typically slightly undulating, with the undulations being regular in both periodicity and intensity. The thickness of the glaze was regular across the surface, being typically around 450μm. Moreover, the glaze displayed no cracks or porosities.

4.2 Contact angle and wettability characteristics

An optical micrograph of a sessile drop of enamel (20^0C) placed on the surface of the mild steel before (a) and after (b) HPDL irradiation with the contact angle superimposed is shown in Fig. 3. As one can see from Fig. 3, HPDL irradiation of the mild steel surface effected a considerable reduction in the enamel contact angle.

One explanation for this observed reduction in the enamel contact angle is that the surface obtained after laser treatment was somewhat smoother than the original untreated surface. The mean surface roughness (Ra) value of the surface of the as-received mild steel was 1.46μm, whilst for the HPDL treated mild steel surface the mean Ra value was 1.12μm. Similar laser induced surface smoothing effects were obtained by Nicolas *et al.* [26] and Henari *et al.* [11], who observed that excimer laser treatment of ceramics and metals could result in the generation of a smoother surface. Thus, according to Eq. (2), the smoother surface will inherently result in a reduction in the contact angle. Indeed, this fact is borne out somewhat by Fig. 4, which shows that the surface condition of the mild steel resulting from HPDL modification (with a number of different traverse speeds) greatly affected the measured contact angle.

As one can see from Fig. 4, at relatively low traverse speeds excess energy is deposited on the surface of the mild steel resulting in a high level of surface melting. This in turn causes porosities and a generally rough surface profile. As the traverse speed increases, however, the energy deposited on the surface of the mild steel reduces. Accordingly the degree of surface melting reduces ultimately to the optimum degree, resulting in the minimum surface roughness, and contact angle, at around 1500 mm/min. Beyond this point the surface roughness, and contact angle, can be seen to increase, indicating that insufficient melting, and consequently smoothing, was achieved.

Such results are in accord with those obtained by Feng *et al.* [27], who noted that under certain surface conditions, contact angle reduction was inversely proportional to surface roughness. Moreover, Olfert *et al.* [12] found that excimer laser treatment of steel surfaces greatly improved the adhesion of a zinc

coating. They asserted that laser treatment occasioned the smoothing of many of the high frequency surface features, resulting in more complete wetting by the zinc.

In addition, the improvement in the wetting action experienced by the mild steel can be ascribed in some part to the increase in the surface O_2 content of the mild steel following HPDL treatment; since this is known to increase the likelihood of wetting [1, 9]. Indeed, since wetting is governed by the first atomic layers of the surface of a material, the O_2 content at the surface of the mild steel before and after HPDL treatment was determined using XPS. The surface oxygen content was found to have increased after HPDL treatment from 34atomic% to 40atomic%. Clearly, oxidisation of the HPDL treated surface of the mild steel has occurred, thus indicating that O_2 enrichment of the laser treated mild steel surface was active in promoting wetting and adhesion [1, 9].

4.3 Mild steel surface energy and its dispersive/polar characteristics

It is possible to estimate the dispersive component of the mild steel's surface energy, γ_{sv}^{d}, by using Eq. (6), and plotting the graph of cos θ against $(\gamma_{lv}^{d})^{1/2}/\gamma_{lv}$ (Fig. 5). Thus the value of γ_{sv}^{d} is estimated by the gradient $(=2(\gamma_{sv}^{d})^{1/2})$ of the line which connects the origin (cos θ = -1) with the intercept point of the straight line (cos θ against $(\gamma_{lv}^{d})^{1/2}/\gamma_{lv}$) correlating the data point with the abscissa at cos θ = 1 [28]. The value of γ_{sv}^{d} for the untreated and HPDL treated (1500 mm/min traverse speed) mild steel is shown in Table 2. From the best-fit plots of cos θ against $(\gamma_{lv}^{d})^{1/2}/\gamma_{lv}$, it was found that the ordinate intercept point of the untreated mild steel-liquid system was closer to cos θ = -1 than that of the HPDL treated mild steel-liquid system. This indicates that, in principle, dispersion forces are acting mainly at the mild steel-liquid interface, resulting in poor adhesion [28, 29]. In contrast, the best-fit straight line for the HPDL treated mild steel-liquid system intercepted the ordinate considerably higher above the origin. This is indicative of the action of polar forces across the interface, in addition to dispersion forces, hence improved wettability and adhesion is promoted [28, 29].

It is not possible to determine the value of the polar component of the mild steel's surface energy, γ_{sv}^{p}, directly from plots of cos θ against $(\gamma_{lv}^{d})^{1/2}/\gamma_{lv}$. This is because the intercept of the straight line (cos θ against $(\gamma_{lv}^{d})^{1/2}/\gamma_{lv}$) is at $2\left(\gamma_{sv}^{p}\gamma_{lv}^{p}\right)^{1/2}/\gamma_{lv}$, and thus only refers to individual control liquids and not the control liquid system. However, it has been established that the entire amount of the surface energies due to dispersion forces either of the solids or the liquids are active in the wettability

performance [28, 30]. It is therefore possible to calculate the dispersive component of the work of adhesion, W_{ad}^{d}, using only the relevant part of Eq. (5) thus

$$W_{ad}^{d} = 2\left(\gamma_{sv}^{d}\gamma_{lv}^{d}\right)^{1/2} \tag{7}$$

The results revealed that for each particular control liquid in contact with both the untreated and laser treated mild steel surfaces, W_{ad} could be correlated with W_{ad}^{d} by the straight line relationship

$$W_{ad} = aW_{ad}^{d} + b \tag{8}$$

where *a* and *b* are constants unique to each control liquid system. Also, for the control test liquids used, a linear relationship between the dispersive and polar components of the control test liquids surface energies has been deduced which satisfies the equation

$$\left(\gamma_{lv}^{p}\right)^{1/2} = 1.3\left(\gamma_{lv}^{d}\right)^{1/2} + 1.15 \tag{9}$$

By introducing Eq. (8) into Eq. (5) and rearranging, then

$$W_{ad}^{p} = (a-1)W_{ad}^{d} + b \tag{10}$$

By combining Eq. (10) with Eq. (5) and differentiating with respect to $\left(\gamma_{lv}^{d}\right)^{1/2}$, then the following can be derived:

$$\left(\gamma_{sv}^{p}\right)^{1/2} = \frac{\left(\gamma_{sv}^{d}\right)^{1/2}(a-1)}{1.3} \tag{11}$$

From a plot of the linear relationship between W_{ad} and W_{ad}^{d}, *a* (the gradient of the relationship between W_{ad} and W_{ad}^{d}) was determined for the untreated and laser treated mild steel. Since γ_{sv}^{d} has already been determined for the untreated and laser treated mild steel from the plots of Eq. (6), it is possible to calculate γ_{sv}^{p} for untreated and laser treated mild steel using Eq. (11) (see Table 2).

As Table 2 shows clearly, HPDL treatment of the surface of the mild steel has led to a small increase in the polar component of the surface energy, γ_{sv}^{p}, thus improving the action of wetting and adhesion.

It is surmised that this increase may be due to HPDL induced changes in the surface microstructure of the mild steel.

It is important to note that because of the long range ionic interactions in the mild steel and the composite nature of the interfaces between the mild steel and the control liquids, it is highly likely that the thermodynamically defined total solid surface energy, γ, as defined in Eq. (4), will be higher than the sum of the dispersive, γ^d, and the polar, γ^p, components of the surface energy. Although the increase in (excess) surface free energy will probably be less than the increase in the total lattice energy. On the other hand an absorbed liquid layer may shield the ionic fields substantially. As such, all the data derived from Eq. (5) - (11) should be considered as being semi-empirical. Notwithstanding this, as the studies by Gutowski *et al.*[6] and Agathopoulos *et al.* [23] found, it is reasonable to conclude from the data obtained from Eq. (5) - (11) that HPDL treatment of the mild steel surface has caused a small increase in the polar component, γ^p, of the surface energy.

4.4 Bonding mechanisms

Based on the nature of the attractive forces existing across a liquid-solid interface, wetting can be classified into the two broad categories of physical wetting and chemical wetting. In physical wetting the attractive energy required to wet a surface is provided by the reversible physical forces (van der Waals). In chemical wetting adhesion is achieved as a result of reactions occurring between the mating surfaces, giving rise to chemical bonds [31].

In practice, complex combinations of various bonding mechanisms actually occur, varying according to the types of materials used [31]. For the mild steel and the enamel, the mechanisms involved in the bonding are principally: physical bonding (van der Waals forces), mechanical bonding, chemical bonding (oxide transformation and O_2 bridging) and on a very small scale, electrochemical reactions such as the electrolytic (redox) effect due to the presence of ferric oxides within the mild steel reacting with other oxides in the enamel [31]. Invariably, the preponderant bonding mechanisms between mild steels and enamels are physical and mechanical bonding [32]. However, an EDX analysis conducted at the interface between the mild steel and the enamel revealed the presence of a small diffusion region which contained elements unique to both the mild steel and the enamel. This is perhaps to be expected since enamel glazes on steels are typically bonded as a result of some of the base material dissolving into the glaze [31], with wetting characteristics often being achieved or enhanced by a reaction at the interface at an elevated temperature [33]. Indeed, when an oxide layer is

present on the surface of a metal, as was the case for the HPDL treated mild steel, then typically the fired enamel dissolves this oxide layer. Subsequently a redox reaction has to occur at the interface to form more metal oxide [33]. In the case of the HPDL treated mild steel and the enamel, which is an Fe/CoO-sodium silicate glass system, then because the oxidation potential for Fe is higher than that for Co, then the redox reaction forms FeO at the interface. Thus a layer of FeO continually remains at the interface and acts as the compatible oxide phase that provides the chemical bonding between the HPDL treated mild steel and the enamel [33]. Additionally, intrinsic within the redox reaction formation of FeO is the alloying of the Fe with the reduced Co to form dendrites in the interfacial zone by means of a microgalvanic cell mechanism [32, 33]. Furthermore, this alloying has a negative free energy which therefore contributes to the driving force for the net redox reaction formation of FeO [33].

As one can see from Fig. 6, there it is not possible to discern any dendritic growth within the enamel glaze in the bond region, which is characteristic of enamels fired onto substrates containing Fe, Si and in particular Co [32]. However, it can be seen that enamel is held firm in the surface irregularities, thus ensuring sound adhesion. Again, such mechanical bonding is typical of enamel glazes on metals [32].

5 CONCLUSION

HPDL surface treatment of the mild steel resulted in changes in the wettability characteristics of the mild steel and the enamel as Table 3 shows.

Improvements in the wetting action of the mild steel after HPDL treatment were identified as being due to:

i. The HPDL induced melting of the mild steel surface which brought about a reduction of the surface roughness, thus directly reducing the contact angle, θ.
ii. The small increase in the polar component of the surface energy, γ_{sv}^{p}, after HPDL treatment (which is thought to be due to the HPDL effected microstructural changes), thus improving the action of wetting and adhesion.
iii. The increase in the surface oxygen content of the mild steel resulting from HPDL treatment was identified as further promoting the action of wetting.

This work demonstrates that it is distinctly possible to alter the wetting characteristics of the selected mild steel using the HPDL.

REFERENCES

1. Ueki, M. Naka, M. & Okamoto, I., Wettability of some metals against zirconia coatings, *J. of Mater. Sci. Lett.* **5** (1986) 1261-2.

2. Nikopoulos, P. & Sotiropoulou, D., Wettability between zirconia ceramics and the liquid metals copper, nickel and cobalt, *J. of Mater. Sci. Lett.* **6** (1987) 1429-30.

3. Chidambaram, P.R., Edwards, G.R. & Olson, D.L., A thermodynamic criterion to predict wettability at metal-alumina interfaces", *Metallurgical Trans. B*, **23B** (1992) 215-22.

4. Li, J.G., Role of electron density of liquid metals and bandgap energy of solid ceramics on the work of adhesion and wettability of metal-ceramic systems, *J. of Mater. Sci. Lett.* **11** (1992) 903-5.

5. Li, J.G., Chemical trends in the thermodynamic adhesion of metal/ceramic systems, *Mater. Lett.* **22** (1995) 169-74.

6. Gutowski, V.W., Russell, L. & Cerra, A., *Adhesion of Silicone Sealants to Organic-Coated Aluminium.* In Klosowski, J.M. (ed). Science and Technology of Building Seals, Sealants, Glazing and Waterproofing, Philadelphia, ASTM, 1992, pp. 144-59.

7. Zhou, X.B. & de Hosson, J.Th.M., Microstructure and interfaces of a reaction coating on aluminium alloys by laser processing, *J. de Physique IV*, **3** (1993) 1007-11.

8. Zhou, X.B. & de Hosson, J.Th.M., Metal-ceramic interfaces in laser coated aluminium alloys, *Acta Metallurgica et Materialia*, **42** (1994) 1155-62.

9. Li, J.G., Microscopic approach of adhesion and wetting of liquid metal on solid ionocovalent oxide surface, *Rare Metals*, **12** (1993) 84-96.

10. Heitz, J., Arenholz E., Kefer T., Bäuerle D., Hibst H. & Hagemeyer A., Enhanced adhesion of metal films on PET after uv-laser treatment, *App. Phys. A* **55** (1992) 391-2

11. Henari, F. & Blau, W., Excimer laser surface treatment of metals for improved adhesion, *App. Optics*, **34** (1995) 581-4.

12. Olfert, M., Duley, W. & North, T., *Laser Treatment for Adhesive Bonding in Coated Steels*. In: Mazumder, J. (ed). Laser Processing, Amsterdam: Kluwer Academic Publishing, 1996, pp. 479-90

13. Lawrence, J. & Li, L., Wettability characteristics of a mild steel modified with CO_2, Nd:YAG, excimer and high power diode lasers, *J. Phys. D,* **32** (1999) 2311-8.

14. Lawrence, J., Li, L. & Spencer, J.T., Ceramic tile grout removal and tile sealing using high power lasers, *Proc. of ICALEO'96: Laser Materials Processing*, Detroit, 1996, pp. 138-48.

15. Lawrence, J., Li, L. & Spencer, J.T., A two-stage ceramic tile grout sealing process using a high power diode laser Part I: Grout development and materials characteristics, *Optics & Laser Tech.* **30** (1998) 205-14.

16. Lawrence, J., Li, L. & Spencer, J.T., A two-stage ceramic tile grout sealing process using a high power diode laser. Part II: Mechanical, chemical and physical properties, *Optics & Laser Tech.* **30** (1998) 215-23.

17. Lawrence, J., PhD Thesis, University of Manchester Institute of Science & Technology (UMIST), 1999.

18. Jaycock, M.J. & Parfitt, G.D., *Chemistry of Interfaces*, London: John Wiley & Sons, 1984.

19. Wenzel, R.N., Resistance of solid surfaces to wetting by water, *Ind. & Eng. Chem.* **28** (1936) 988-94.

20. Cassie, A.B.D., Baxter, S., Wettability of porous surfaces, *Trans. Faraday Soc.* **40** (1944) 546-51.

21. Zhou, X.B., De Hosson, J.Th.M., Influence of surface roughness on the wetting angle, *J. Mater. Res.* **10** (1995) 1984-92.

22. Neumann, A.W., Good, R.J., Thermodynamics of contact angles. I: Heterogeneous solid surfaces, *J. Colloid and Interface Sci.* **38** (1972) 341-58.

23. Agathopoulos, S. & Nikolopoulos, P., Wettability and interfacial interactions in bioceramic-body-liquid systems, *J. of Biomedical Mater. Res.* **29** (1995) 421-9.

24. Bourell, D.L., Marcus, H.L., Barlow, J.W. & Beaman, J.J., Selective laser sintering of metals and ceramics, *Int. J. Powder Metallurgy*, **28** (1992) 369-81.

25. Agarwala, M., Bourell, D.L., Beaman, J.J., Marcus, H.L. & Barlow, J.W., Direct laser sintering of metals", *Rapid Prototyping J.* **1** (1995) 26-36.

26. Nicolas, G., Autric, M., Marine, W. & Shafeev, G.A., Laser induced surface modifications on ZrO_2 ceramics, *App. Surf. Sci.*, **109-110** (1997) 289-92.

27. Feng, A., McCoy, B.J., Munir, M.A. & Cagliostro, D., Wettability of transition metal oxide surfaces, *Mater. Sci. & Eng. A*, **1-2** (1998) 50-6.

28. Fowkes, F.M., Attractive forces at interfaces, *Ind. & Eng. Chem.* **56** (1964) 40-52.

29. Chattoraj, D.K. & Birdi, K.S., *Adsorption and the Gibbs Surface Excess*, New York: Plenum Press, 1984, p 95.

30. Girifalco, L.A. & Good, D.J., A theory for the estimation of surface and interfacial energies. III: Estimation of surface energies of solids from contact angle data, *J. of Physical Chem.* **64** (1960) 561-5.

31. Greenhut, V.A., *Surface Considerations for Joining Ceramics and Glasses*, In: Brinson, H.F. (ed) Engineered Materials Handbook: Adhesives and Sealants, Metals Park: ASM International, 1991, pp. 298-311.

32. Vargin, V.V., *Technology of Vitreous Enamels*, New York: Academic Press, 1968.

33. Pask, J.A. & Tomisa, A.P., *Wetting, Surface Energies, Adhesion and Interface Reaction Thermodynamics*, In Schneider, S.J. (ed), Engineered Materials Handbook: Ceramics and Glasses, Metals Park : ASM International, 1991, pp. 482-92.

List of Figs.

Fig. 1

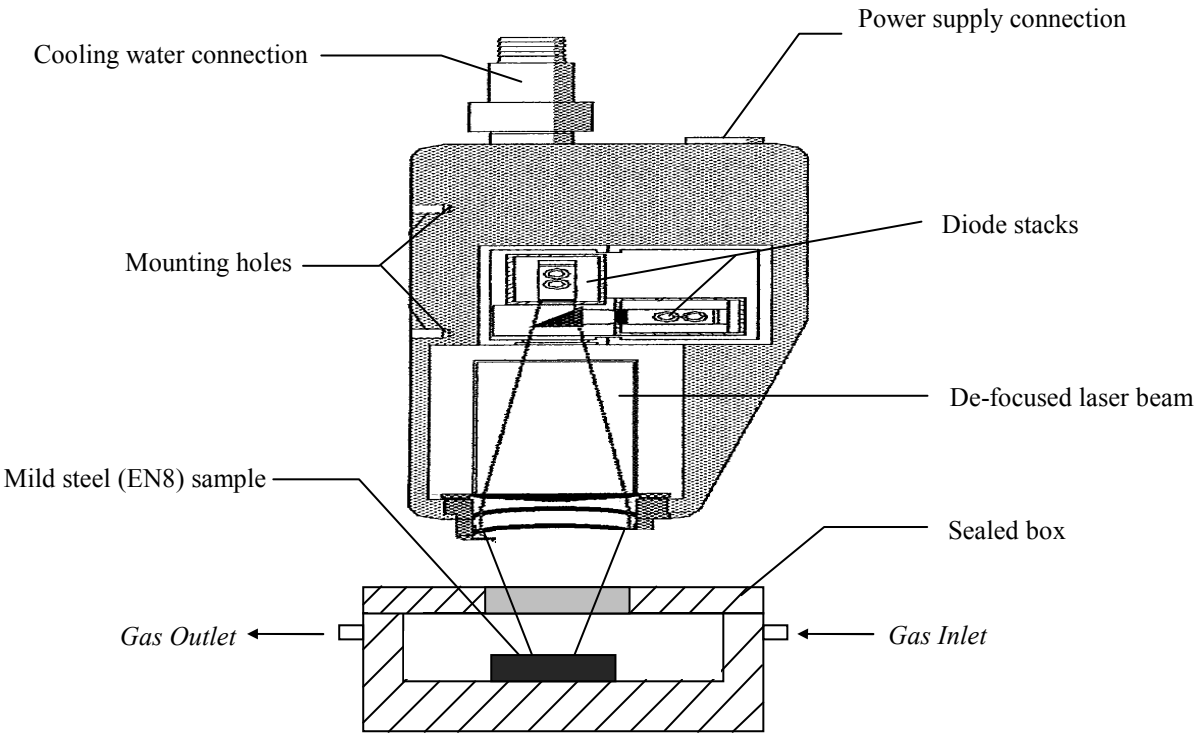
Power supply connection
Cooling water connection
Diode stacks
Mounting holes
De-focused laser beam
Mild steel (EN8) sample
Sealed box
Gas Outlet
Gas Inlet

Fig. 2

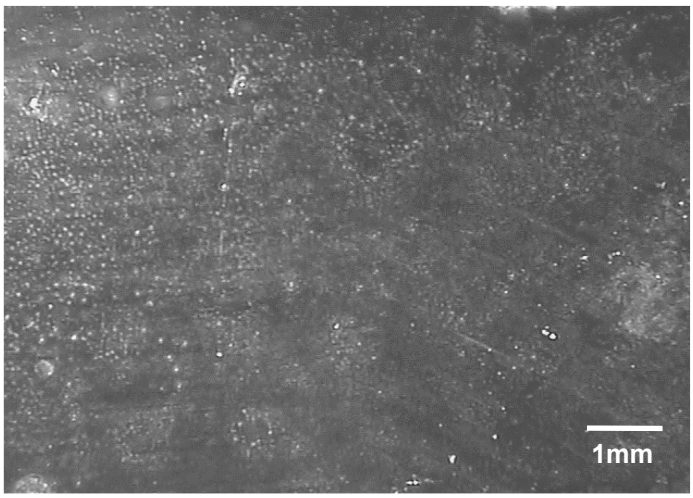

Fig. 3

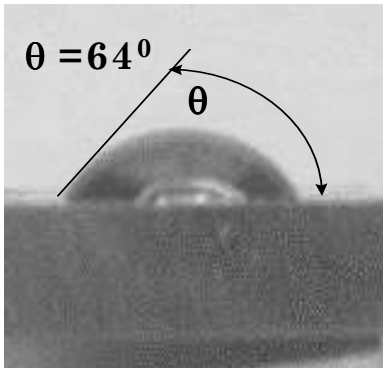

(a)

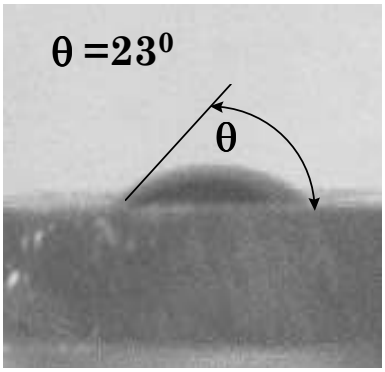

(b)

Fig. 4

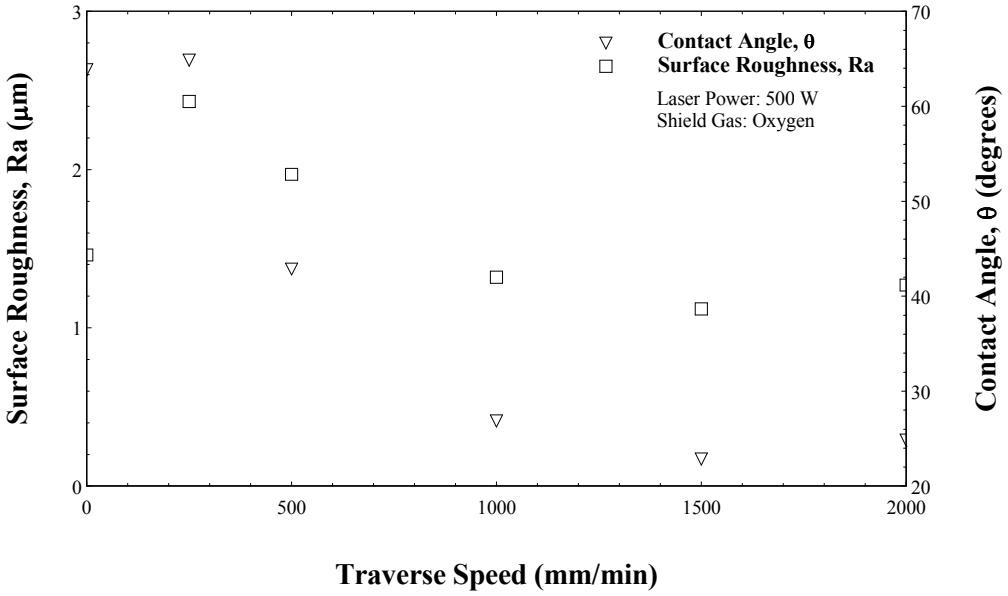
Surface Roughness, Ra (μm)
Contact Angle, θ (degrees)
Traverse Speed (mm/min)
Contact Angle, θ
Surface Roughness, Ra
Laser Power: 500 W
Shield Gas: Oxygen
0
1
2
3
20
30
40
50
60
70
0
500
1000
1500
2000

Fig. 5

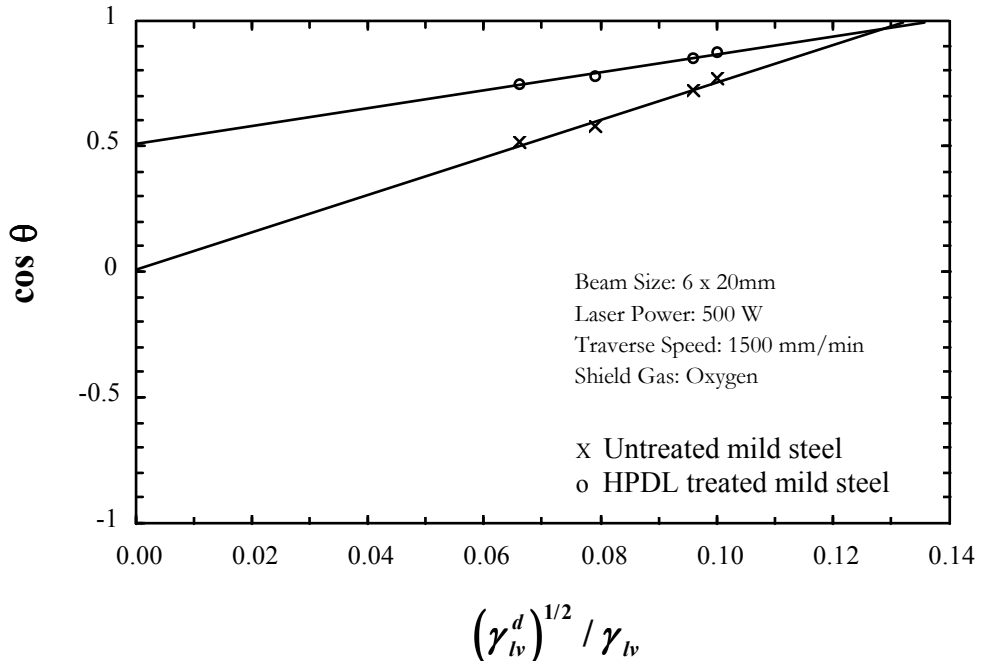
1
0.5
0
-0.5
-1
cos θ
0.00
0.02
0.04
0.06
0.08
0.10
0.12
0.14
$\left(\gamma_{lv}^{d}\right)^{1/2} / \gamma_{lv}$
Beam Size: 6 x 20mm
Laser Power: 500 W
Traverse Speed: 1500 mm/min
Shield Gas: Oxygen
x Untreated mild steel
o HPDL treated mild steel

Fig. 6

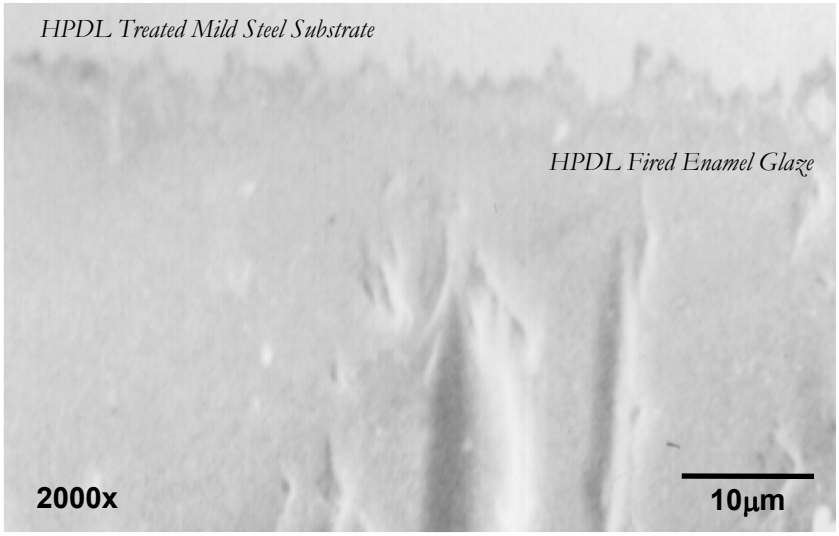
HPDL Treated Mild Steel Substrate
HPDL Fired Enamel Glaze
2000x
10μm

List of Tables

Table 1

Liquid	γ **(mJ/m^2)**	γ_{lv}^{d} **(mJ/m^2)**	γ_{lv}^{p} **(mJ/m^2)**
Human Blood	47.5	11.2	36.3
Human Blood Plasma	50.5	11.0	39.5
Glycerol	63.4	37.0	26.4
4-Octanol	27.5	7.4	20.1

Table 2

Surface Energy Characteristic	Untreated Mild Steel	HPDL Treated Mild Steel
Dispersive Component, (γ_{sv}^{d})	64.6 mJ/m^2	66.2 mJ/m^2
Polar Component, (γ_{sv}^{p})	4.2 mJ/m^2	6.6 mJ/m^2

Table 3

Characteristics	Untreated Mild Steel	HPDL Treated Mild Steel
Contact Angle	64^{o}	23^{o}
Surface Roughness (Ra)	1.46μm	1.12μm
Relative Oxygen Content	34%	40%
Dispersive Component, (γ_{sv}^{d})	64.6 mJ/m^2	66.2 mJ/m^2
Polar Component, (γ_{sv}^{p})	4.2 mJ/m^2	6.6 mJ/m^2